Transactions of the **14th International Conference on Structural Mechanics in Reactor Technology** (SMiRT 14), Lyon, France, August 17-22, 1997 **HKW/4**

An ultimate seismic response analysis of a RC shear wall using a macroscopic model

Moon I.H., Lee K.S., Lee Y.I., Kim S.G.
Korea Power Engineering Company, Korea

ABSTRACT: A seismic ultimate dynamic response test for a reinforced concrete shear wall is simulated by numerical analysis. The shear wall structure is idealized as a macroscopic model which is composed of three vertical line elements connecting two rigid horizontal beams. Three hysteresis models describing the force-displacement relationship of each line element are adopted. A nonlinear analysis computer program SINDAS is developed for this study. Analysis results agree well with test results.

1. INTRODUCTION

Many nuclear power plant structures are composed of reinforced concrete shear wall structures acting as main seismic resisting system. The evaluation of the ultimate strength and seismic responses are important to assess the seismic safety and reliability of these structures.

A seismic ultimate dynamic response test for a reinforced concrete shear wall was carried out by NUPEC in Japan in 1991. The test results were proposed as an International Standard Problem, so called "SSWISP", by OCED/NEA. The main purpose of SSWISP is to clarify the behavior of a concrete shear wall up to its ultimate state, and to improve the reliability of nonlinear seismic analysis codes.[1]

For this study, a macroscopic model having three vertical line elements is constructed, and three hysteresis models are adopted for each line element. A nonlinear dynamic analysis computer program SINDAS is developed using the relationship between the mechanical and the hysteresis model and is used for simulating the seismic ultimate shear wall test results.

2. DESCRIPTION OF SEISMIC ULTIMATE TEST FOR SHEAR WALL

The test specimen of the seismic shear wall is composed of a web wall, a flange wall at each end of the web wall, and top and bottom thick slabs as shown in Fig. 1.

The test was divided into 6 steps for better understanding the response behavior of shear wall at levels ranging from elastic to ultimate state as shown in Fig. 2. Acceleration and displacement responses are measured at several points in the walls and top slab.

The basic seismic input motion as shown in Fig. 3 is applied in the longitudinal direction of the specimen after scaling to produce the proper strain level.

3. DESCRIPTION OF ANALYTICAL MODEL

3.1 Mechanical Model

A macroscopic model idealizing the seismic shear wall structure is shown in Fig. 4. This model is composed of three vertical line elements with infinite rigid beams at the top and bottom slab levels. The two side elements are truss elements which represent the axial stiffness of the flange walls. The central element representing the web wall is a one component model having vertical, horizontal, and rotational springs concentrated at the base. A finite rigid element having a length of ch is placed between the spring assembly and the lower rigid beam. The location of relative rotation center, c is assumed to be 0.2. An effective flange wall length is assumed to be $b_{eff} = h/3$ according to Gupta's study[2].

This model is capable of describing the flexural and shear deformation except for deformations due to fixed end rotation. Furthermore, this model can simulate the flexural and sliding shear modes at failure condition, but can not simulate the web splitting-crushing mode at the failure state.

3.2 Hysteresis Models

Vertical Spring of Web Wall

An axial stiffness hysteresis model shown in Fig. 5 [3] is used to describe the axial force-deformation relationship of the vertical spring used in the web wall. The skeleton curve is defined by assuming the axial stiffness ($K_c = K_{aw}$) to be constant in compression. Tension stiffness (K_t) is reduced to 90% of the initial compressive elastic stiffness in order to account for some stiffness degradation due to cracking and bond deterioration. After tensile yielding, the stiffness(K_h) is reduced to 0.1% of the initial elastic stiffness in order to represent some strain hardening.

Horizontal and Rotational Spring of Web Wall

The origin oriented hysteresis model as shown in Fig. 6 [3] is used for both horizontal and rotational springs of the web wall. The characteristic of this model is small dissipation of hysteresis energy. A trilinear skeleton curve is used for both rotational and horizontal springs. The shear stiffness degradation is taken without accounting for cracking effects due to the presence of both actual axial force and bending moment.

The stiffness value of the horizontal spring(K_{hw}, Fig.1) in the initial elastic range represents the shear stiffness of the wall in this range, which was defined by inducing a shape factor for shear deformation proposed by Tomii and Osaki[4].

The stiffness properties of the rotational spring (K_r) are defined by referring to the wall area bounded by the inner faces of the two flanges. The bending moment is assumed to be distributed uniformly along the story height with an amplitude equal to the moment at the critical section of the wall. The properties of the rotational spring are defined by a moment-curvature analysis based on displacement compatibility. The moment-curvature relationship ($M - \phi$) is idealized as a trilinear curve and simulated by the origin oriented hysteresis model under cyclic loading.

Because of shear wall deterioration due to cracking and bond slip, the stiffness of horizontal and rotational springs are reduced at the next run step after the previous run step finished in the nonlinear range. The unloading spring stiffness of the previous run step is used for the spring stiffness of the next run step in order to consider reduced stiffness due to cracking and bond slip.

Vertical Spring of Flange Wall

A simplified axial stiffness hysteresis model is proposed to describe the relationship of the axial force and deformation of the flange wall. This model is basically the same as the axial stiffness hysteresis model with the exception that, when the loading decreases after tensile yielding, the response point follows the initial elastic stiffness in tension. (Fig. 7)

The axial stiffness properties of the flange truss elements are defined as an independent column by referring to the area of the boundary elements. The axial stiffness properties of the flange truss elements are defined as an independent column by referring to the area of the boundary elements.

3.3 Mathematical Model

The hysteretic models of flexural, shear, and axial springs in the mechanical model can be used to drive the elastic stiffnesses of these springs at any step in the loading history. Consequently, these stiffnesses can be used in constructing the overall elastic stiffness matrix of the element.

The elastic stiffness of the web wall, K_e can be calculated by using the relationship between displacement and loading at midpoint of the top and the bottom rigid beams. That is, the elastic stiffness matrix can be calculated from the assumption of finite element with *ch* length shown in Fig. 4 and the elastic energy equation as Equation (1).

$$K_e = \begin{bmatrix} K_{hw} & 0 & K_{hw}(1-c)h & -K_{hw} & 0 & K_{hw}ch \\ & K_{aw} & 0 & 0 & -K_{aw} & 0 \\ & & K_{rw}+K_{hw}(1-c)^2h^2 & K_{hw}(c-1)h & 0 & -K_{rw}-K_{hw}c(c-1)h^2 \\ & & & K_{hw} & 0 & -K_{hw}ch \\ & & SYMMETRIC & & K_{aw} & 0 \\ & & & & & K_{rw}+K_{hw}(ch)^2 \end{bmatrix} \quad (1)$$

Equation (1) is the relation at the midpoint of the rigid beams. The stiffness matrix (K_f) related to displacement at four ends of the rigid beam can be obtained as Equation (2).

$$[K_f] = [B]^T [K_e][B] \quad (2)$$

where, $[B]$ = the displacement transformation matrix in order to calculate the stiffness matrix at the ends of the rigid beam.

The stiffness matrix of the flange wall idealized as a truss element can be calculated by Equation (3).

$$K_{af}\begin{bmatrix} 1 & -1 \\ -1 & 1 \end{bmatrix}\begin{bmatrix} U_i \\ U_i \end{bmatrix} = \begin{bmatrix} F_i \\ F_i \end{bmatrix} \quad (3)$$

where F_i = member force

3.4 Damping Values

Rayleigh damping is used in the dynamic analysis. The parameters α and β are estimated from the natural frequency resulting from frequency analysis and assumed equivalent damping ratio. Assumed equivalent damping ratios are 1% for RUN-1 and RUN-2, 2% for RUN-2' and RUN-3, 3% for RUN-4, and 4% for RUN-5.

3.5 Computer Program

The computer program SINDAS is developed for this study. The program SINDAS deals with nonlinear static and dynamic problems having both material and geometrical nonlinearity for a reinforced concrete shear wall. The nonlinear analysis algorithm used in the program is based on Newmark's linear acceleration method and the modified Newton-Raphson iterative solution method. The criteria used to establish convergence of iterations is based on force tolerance and energy tolerance.

4. ANALYTICAL RESULTS

Analytical responses are compared with test results at a top slab location, and show in Tables 1 through 3 and Figures 8 and 10. Analytical response time histories generally match with the test results up to test step RUN-4 and a portion of RUN-5.

However, analytical response time histories after 4 seconds for RUN-5 (Fig. 9, (c)) become smaller and shorter than those of the actual test results. The comparison of hysteresis loops are quite different from each other as shown in Fig. 11. These differences are due to the characteristics of the analytical model used in this study that can not properly simulate the splitting-crushing mode of web wall at the failure state.

5. CONCLUSIONS

As a part of the Seismic Shear Wall International Standard Problem proposed by OECD/NEA, the seismic ultimate dynamic test results for a shear wall is simulated by nonlinear dynamic analyses. A macroscopic model composed of three vertical line elements having three hysteresis models is constructed and analyzed using the computer program SINDAS which is developed for this study.

The analytical responses match well with the test results. The following conclusions are made from the study.

(1) The macroscopic model is useful for prediction of nonlinear behavior of the shear wall subjected to seismic strong motion.

(2) The three vertical line element model is useful for nonlinear dynamic analysis of a squat shear wall. However, this model can not properly simulate the splitting-crushing mode at the failure state.

(3) An appropriate effective flange length should be used for estimating the stiffness of the flange wall.

(4) The shear deformation of squat shear wall is dominant for total deformation

ACKNOWLEDGEMENT: This study is performed as a part of Seismic Shear Wall International Standard Problem proposed by OECD/NEA/CNSI and NUPEC, Japan.

REFERENCES

1. OECD/NEA & NUPEC 1994. *Specification Report of Seismic Shear Wall ISP on NUPEC's Seismic Ultimate Dynamic Response Test.*
2. Gupta, A.J. 1984. Modeling of Shear Wall Buildings. *Nuclear Engineering and Design* 79: 69-80.
3. Kabeyasawa, H., H. Shioara, S. Otani & H. Aoyama 1982. Analysis of the Full-Scale Seven-Story Reinforced Concrete Test Structures: Test PSD3, *Proc. 3rd Joint Technical Coordinating Committee*, US-Japan Cooperative Earthquake Research Program. Building Research Institute: Tsukuba, Japan
4. Tomii, M. and Y. Osaki 1975. Shearing Resistance of Reinforced Concrete Shear Walls and Analysis on Them (in Japan). *Kenchiku Kenkyu Shiryo* 6. Building Research Institute: Ministry of Construction, Japan

Table 1. Natural Frequencies

Step	Test	Analysis
Initial	13.20 Hz	11.50 Hz
RUN-3	10.55 Hz	10.55 Hz
RUN-4	8.74 Hz	8.74 Hz
RUN-5	8.34 Hz	8.35 Hz

Table 2. Maximum Displacements

Step	Test		Analysis	
	Time(sec)	Disp.(mm)	Time(sec)	Disp.(mm)
RUN-3	2.825	1.630	2.820	1.780
RUN-4	4.525	3.706	4.515	3.850
RUN-5	3.710	15.002	3.825	22.100

Table 3. Maximum Accelerations at Top Slab

Step	Test		Analysis	
	Time(sec)	Disp.(gal)	Time(sec)	Disp.(gal)
RUN-3	2.820	704.385	2.820	722.0
RUN-4	4.515	877.680	4.510	877.0
RUN-5	3.795	1,336.610	3.815	1,200.0

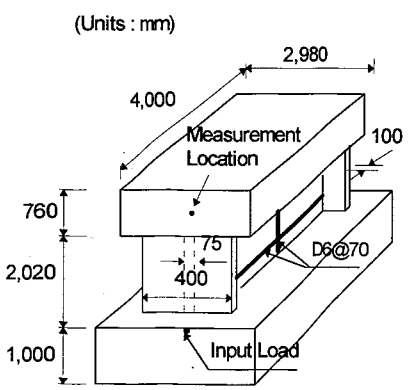

Figure 1. Geometry of Test Specimen

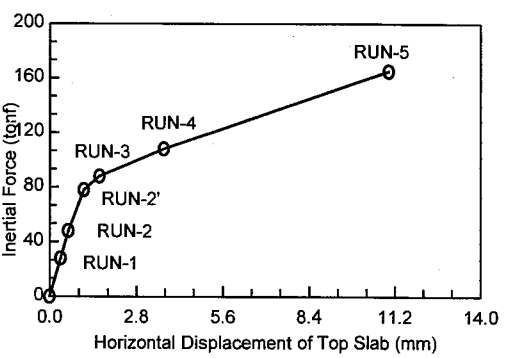

Figure 2. Six Target Levels of Response

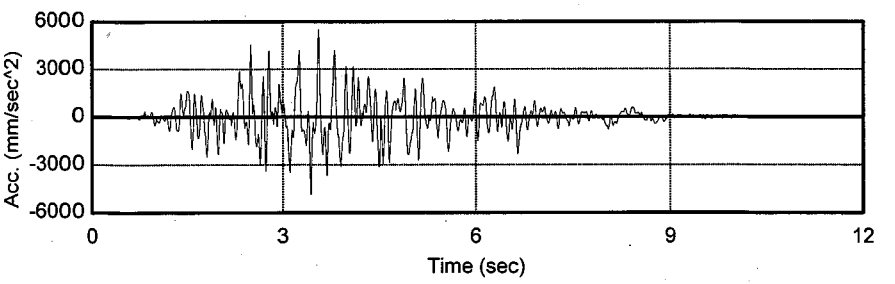

Figure 3. Seismic Input Motion

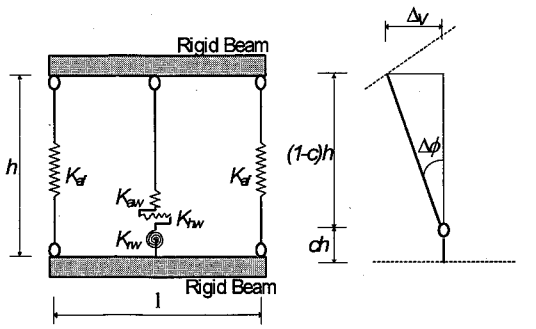

Figure 4. Mechanical Model

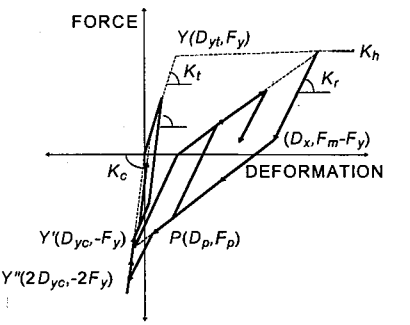

Figure 5. Axial Stiffness Hysteresis Model

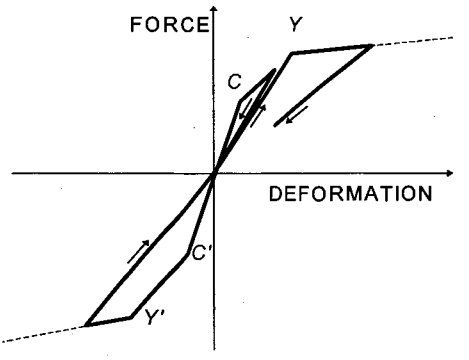

Figure 6. Origin Oriented Hysteresis Model

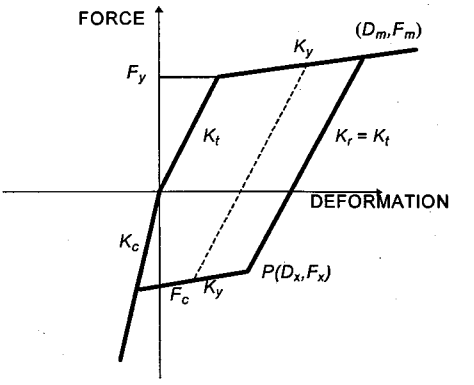

Figure 7. Simplified Axial Stiffness Hysteresis Model

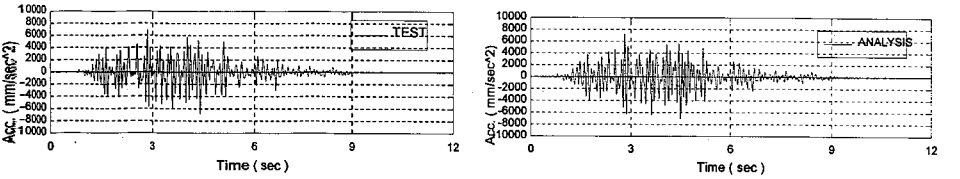

(a) RUN-3

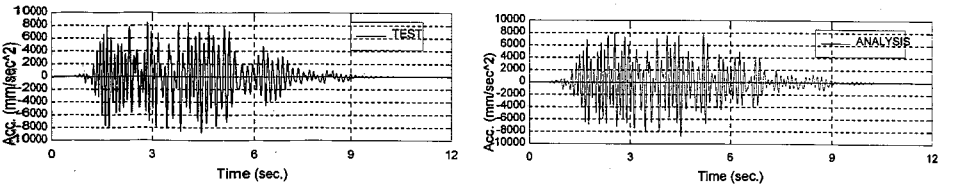

(b) RUN-4

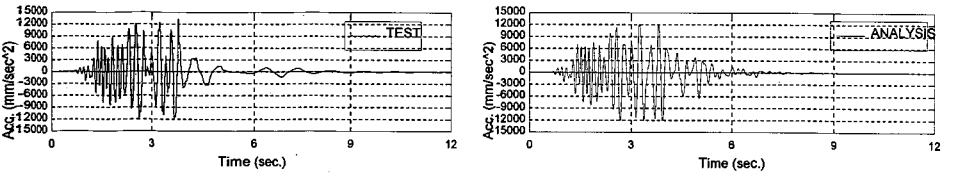

(c) RUN-5

Figure 8. Horizontal Acceleration Response Time Histories at Top Slab

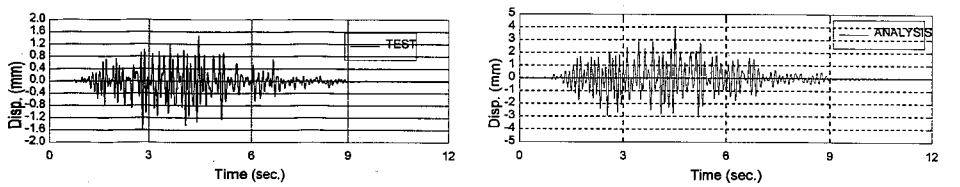

(a) RUN-3

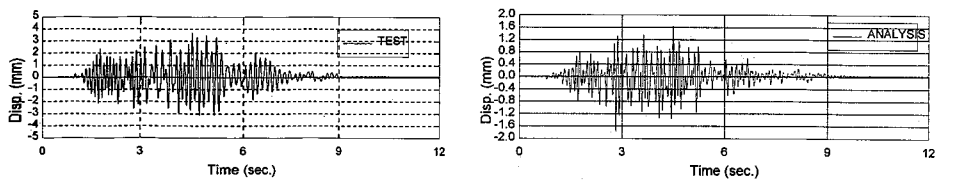

(b) RUN-4

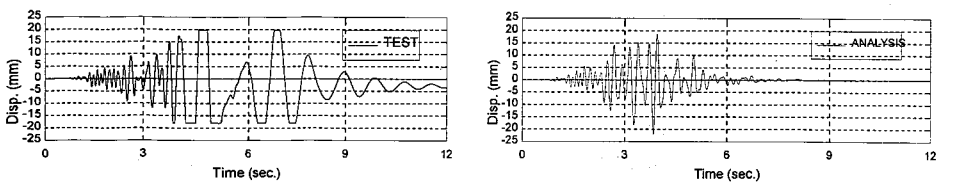

(c) RUN-5

Figure 9. Horizontal Displacement Response Time Histories at Top Slab

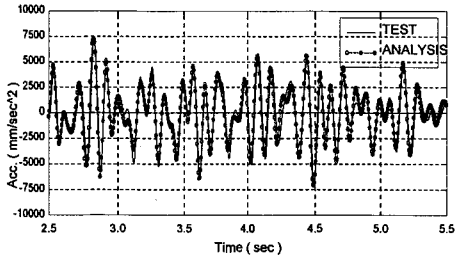

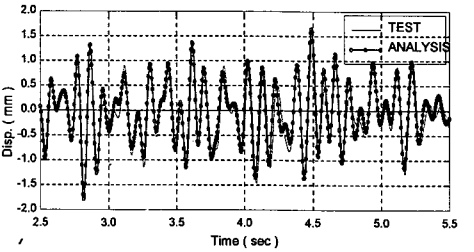

(a) Acceleration & Displacement (RUN-3 : 2.5sec - 5.5sec)

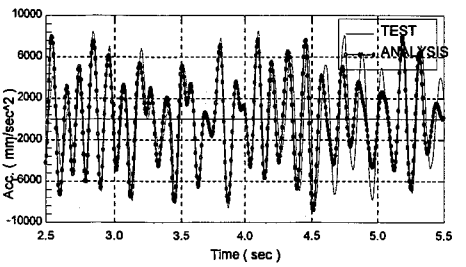

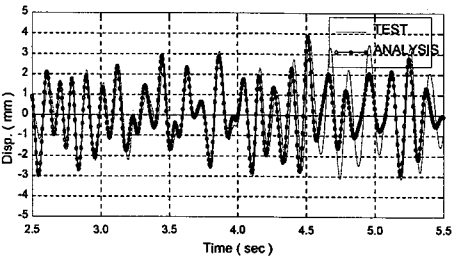

(b) Acceleration & Displacement (RUN-4 : 2.5sec - 5.5sec)

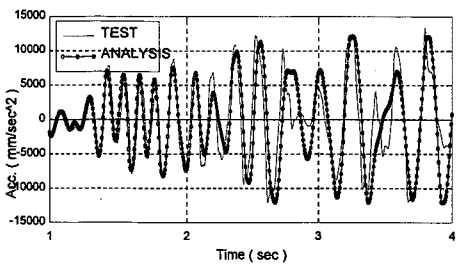

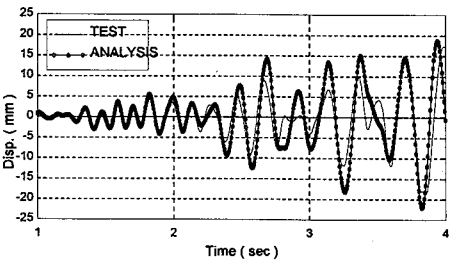

(c) Acceleration & Displacement (RUN-5 : 1.0sec - 4sec)

Figure 10. Detailed Comparisons of Horizontal Time Histories in Strong Motion Range

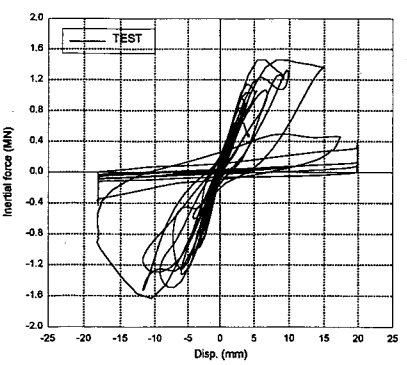

(a) Test

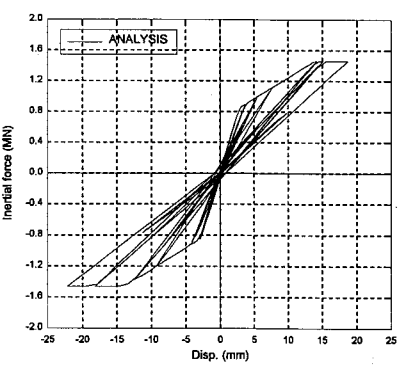

(b) Analysis

Figure 11. Comparison of Hysteresis Loop of RUN-5